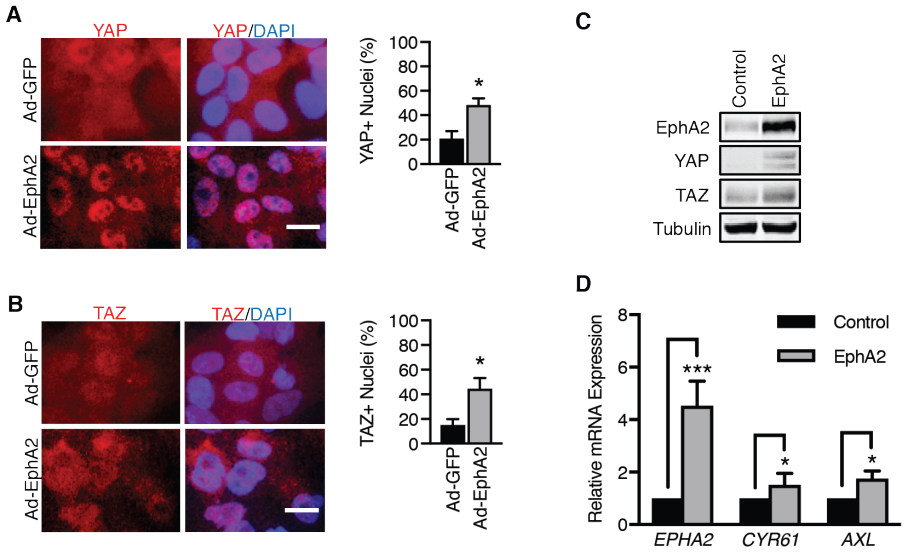

Supplemental Figure 1. EphA2 activates YAP/TAZ in MCF10A-HER2 cells. A,B) Immunofluorescence of (A) YAP or (B) TAZ (both red) in MCF10A-HER2 cells infected with Ad-GFP or Ad-EphA2. Nuclei were stained with DAPI (blue). The percentage of nuclei with YAP or TAZ nuclear localization (YAP+ or TAZ+) were determined using ImageJ software. Data were compiled from three views per sample and three independent experiments. Error bars are SEM, and scale bars are 10 µm. *$p<0.05$; Student's t-test. C) Western blot of EphA2 overexpression in MCF10A-HER2-EphA2 cells. D) Relative mRNA expression was measured in MCF10A-HER2 ("Control") or MCF10A-HER2-EphA2 ("EphA2") cells by qRT-PCR from five independent experiments. Error bars are SEM. *$p<0.05$, ***$p<0.005$; Student's t-test.

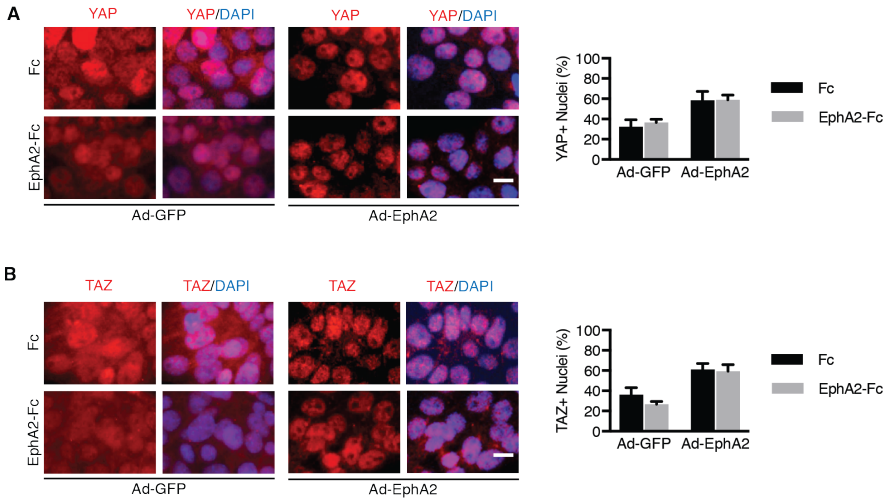

Supplemental Figure 2. EphA2-EphrinA1 interactions do not significantly contribute to YAP/TAZ activation. A,B) Immunofluorescence of (A) YAP or (B) TAZ in *MMTV-Neu* cells infected with Ad-GFP or Ad-EphA2 followed by incubation with the control Fc or a EphA2-Fc chimeric protein. YAP or TAZ positive nuclei were counted using three fields of view from three independent experiments. Error bars are SEM, and scale bars are 10 µm.

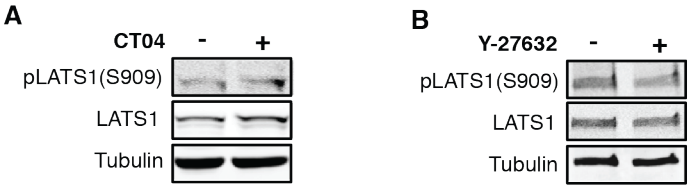

Supplemental Figure 3. Rho and ROCK inhibition did not enhance LATS1 phosphorylation in *MMTV-Neu* cells. Western blot analysis of *MMTV-Neu* cells treated with PBS control, (A) CT04 (3 μg/mL), or (B) Y-27632 (10 μM) for 6 hrs.

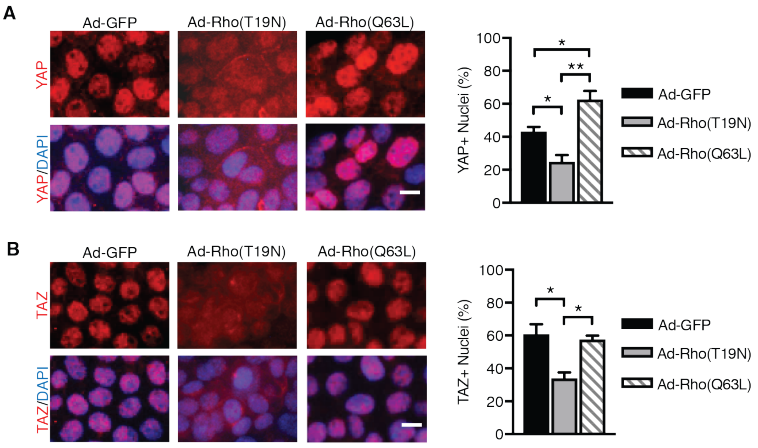

Supplemental Figure 4. EphA2-mediated YAP/TAZ activation requires Rho catalytic activity. Immunofluorescence of (A) YAP or (B) TAZ (both red) and DAPI (blue) in *MMTV-Neu* cells infected with Ad-EphA2 and Ad-GFP, Ad-Rho(T19N), or Ad-Rho(Q63L). Scale bar is 10 µm. DAPI-stained nuclei were counted in ImageJ, and YAP- or TAZ-positive nuclei were counted using at least two fields of view in three independent experiments. Error bars are SEM. *$p<0.05$, **$p<0.01$; one-way ANOVA, Tukey's post hoc.

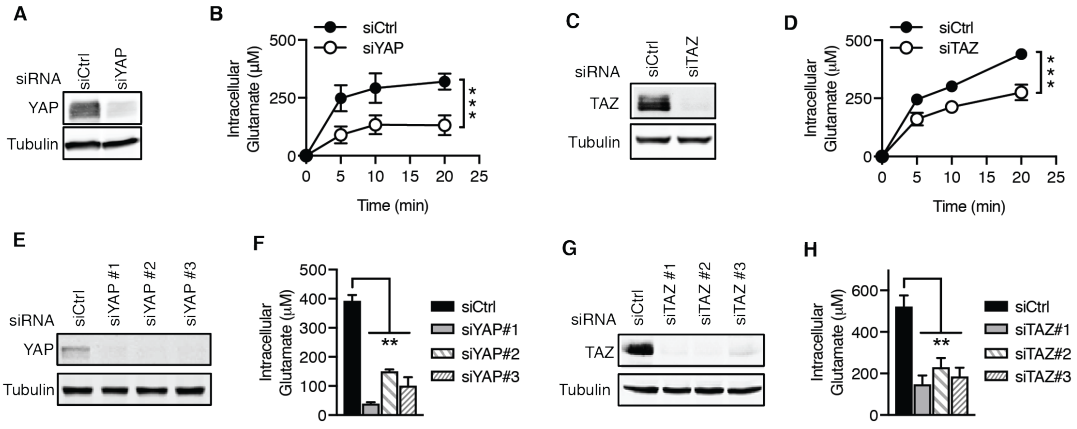

Supplemental Figure 5. YAP and TAZ promote glutamine metabolism in MCF10A-HER2-EphA2 cells. A,C) *YAP* (A) or *TAZ* (C) knockdown using pooled siRNAs in MCF10A-HER2-EphA2 cells by Western blot. Non- targeting (siCtrl) siRNA was used as a control. B,D) Intracellular glutamate concentration (μM) measured at 0, 5, 10, and 20 min after addition of serum (5%), EGF (20 ng/mL), and L-glutamine (2.5 mM) in cells described in (B) and (D). Data from three independent experiments was normalized to the 0 min time point, and error bars are SEM. ***$p<0.005$; two-way ANOVA. E,G) Western blot analysis to demonstrate (E) YAP or (G) TAZ knockdown in MCF10A-HER2-EphA2 cells transfected with individual siRNAs. Control cells were transfected with a non-targeting (siCtrl) control. F,H) Intracellular glutamate concentration (μM) measured 20 minutes after addition of serum (5%), EGF (20 ng/mL), and L-glutamine (2.5 mM) in cells described in (E) and (G). Error bars are SEM calculated from three independent experiments. **$p<0.01$; one-way ANOVA; Dunnett's post hoc.

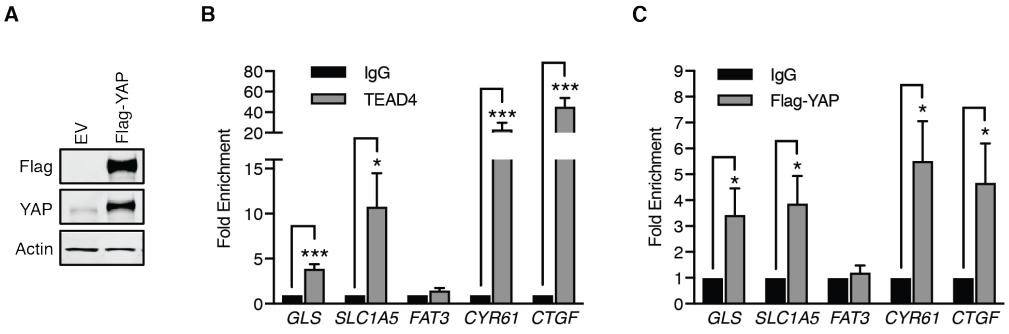

Supplemental Figure 6. YAP and TEAD4 are associated with *GLS* and *SLC1A5* promoters. A) Western blot of Flag-YAP overexpression in MCF10A-HER2 cells. Actin was assessed as a loading control. B,C) Chromatin immunoprecipitation of MCF10A-HER2 cells transduced to express Flag-YAP. Relative immunoprecipitated genomic DNA using (B) TEAD4 or (C) Flag was determined by qRT-PCR and normalized to IgG controls from six independent experiments. Error bars represent SEM. *$p<0.05$, ***$p<0.005$; Student's t-test.

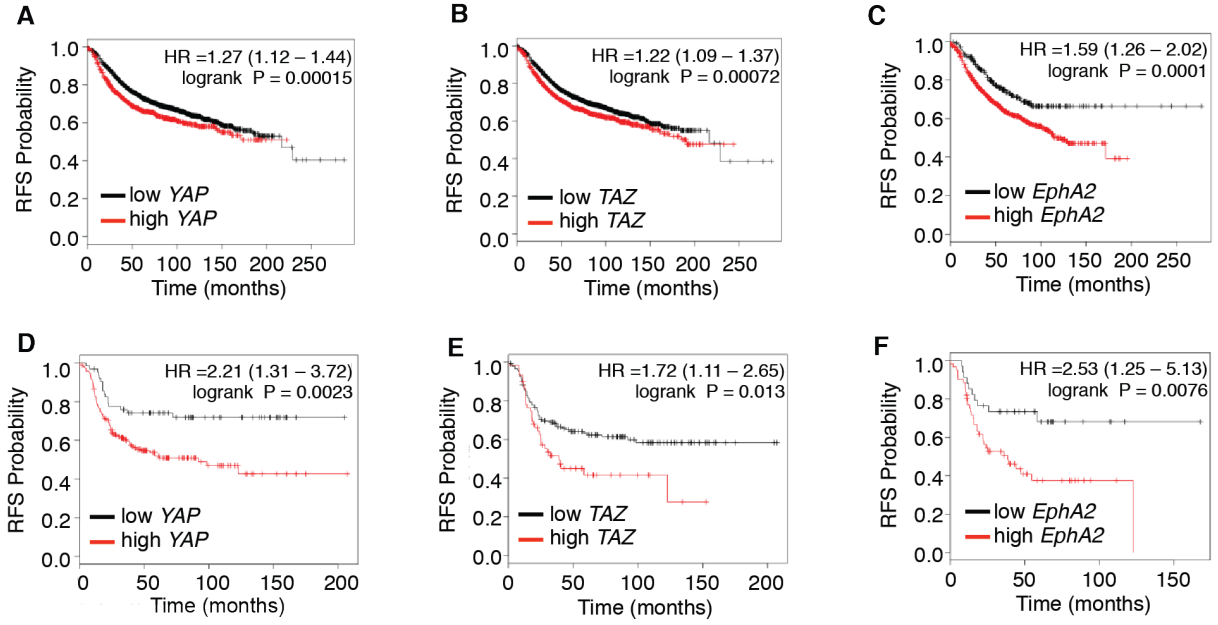

Supplemental Figure 7. *YAP/TAZ* and *EphA2* expression strongly correlate with decreased patient survival in HER2+ breast cancer. Kaplan-Meier analysis of recurrence-free survival (RFS) in (A-C) all or (D-F) only HER2+ breast cancer patients exhibiting low (black) or high (red) expression of (A,D) *YAP* (all: n=1764; HER2+: n=156), (B,E) *TAZ* (all: n=3951; HER2+: n=251), or (C,F) *EphA2* (all: n=1133; HER2+: n=95 in lymph-node positive patients only).

Supplemental Table 1. ChIP Primers

Gene	Forward Primer	Reverse Primer
GLS	AGGCACGTGTAGAGCCATCT	AGCTGGTCCCTTATGCAAAC
SLC1A5	GTGCTAGCCCTGAGGCATTG	ATGCAAGCTGTCCAGGGTAT
FAT3*	GGCTTCCACTTCACACATTCC	TGCCCATTCTACTCTGGCTGTT
CYR61*	CACACACAAAGGTGCAATGGAG	CCGGAGCCCGCCTTTTATAC
CTGF†	GGAGTGGTGCGAAGAGGATA	GCCAATGAGCTGAATGGAGT

* Zancanato F *et al*. *Nature Cell Biology* 17: 1218-1227 (2015).
† Zhang H *et al*. *J Biol Chem* 284: 13355-13362 (2009).

Supplemental Video 1. EphA2 overexpression leads to intranuclear accumulation of YAP. Super-resolution microscopy of YAP subcellular localization in a *MMTV-Neu* cell infected with Ad-GFP (left) or Ad-EphA2 (right). DAPI nuclear stain (blue) and YAP immunofluorescence (red) are shown. Each 2D image is shown along the x-y plane, with signal intensity plotted along the z-axis. The video loop was compiled in ImageJ using six consecutive z-stack images.

Supplemental Video 2. Nuclear exclusion of YAP upon Rho inhibition. Super-resolution microscopy of YAP subcellular localization in a *MMTV-Neu* cell infected with Ad-EphA2 and treated with PBS (Control; left) or (CT04 3 μg/mL for 4 hrs; right). DAPI nuclear stain (blue) and YAP immunofluorescence (red) are shown. Each 2D image is shown along the x-y plane, with signal intensity plotted along the z-axis. The video loop was compiled in ImageJ using seven consecutive z-stack images.